PAPER

Stochastic Geometry Analysis of Inversely Proportional Carrier Sense Threshold and Transmission Power for WLAN Spatial Reuse*

Koji YAMAMOTO[†a)], ***Senior Member***, **Takayuki NISHIO**[††], ***Member***, **Masahiro MORIKURA**[†], ***Fellow***, ***and*** **Hirantha ABEYSEKERA**[†††], ***Member***

SUMMARY In this paper, a stochasic geometry analysis of the inversely proportional setting (IPS) of carrier sense threshold (CST) and transmission power for densely deployed wireless local area networks (WLANs) is presented. In densely deployed WLANs, CST adjustment is a crucial technology to enhance spatial reuse, but it can starve surrounding transmitters due to an asymmetric carrier sensing relationship. In order for the carrier sensing relationship to be symmetric, the IPS of the CST and transmission power is a promising approach, i.e., each transmitter jointly adjusts its CST and transmission power in order for their product to be equal to those of others. This setting is used for spatial reuse in IEEE 802.11ax. By assuming that the set of potential transmitters follows a Poisson point process, the impact of the IPS on throughput is formulated based on stochastic geometry in two scenarios: an adjustment at a single transmitter and an identical adjustment at all transmitters. The asymptotic expression of the throughput in dense WLANs is derived and an explicit solution of the optimal CST is achieved as a function of the number of neighboring potential transmitters and signal-to-interference power ratio using approximations. This solution was confirmed through numerical results, where the explicit solution achieved throughput penalties of less than 8% relative to the numerically evaluated optimal solution.

key words: *IEEE 802.11ax, spatial reuse, carrier sense threshold, stochastic geometry*

1. Introduction

The proliferation of wireless local area networks (WLANs) has led to the dense deployment of access points (APs). However, in such environments, APs and stations (STAs) experience substantial interference from neighboring APs and STAs, i.e., overlapping basic service sets (OBSSs). Due to the carrier sense multiple access with collision avoidance (CSMA/CA) mechanism, they time-share the channel with all neighboring APs and STAs.

To facilitate spatial channel reuse and improve system throughput, an adjustment to the carrier sense threshold (CST), the so-called clear channel assessment (CCA) threshold [1], of an AP/STA is a promising approach [2], [3]. When the CST is tuned to be greater than interference from neighbors, APs can transmit signals even when their neighbors are transmitting. However, the increased CST increases interference at the AP and the intended STA as well as at neighboring APs/STAs. In addition, the asymmetric carrier sensing relationship resulting from the CST settings can cause throughput starvation at other APs and STAs [4].

We discuss by introducing a rough example shown in Fig. 1, where two APs 1 and 2 separated by 16 m attempt to transmit to their associated STAs using the same channel. Let transmission power and CST of AP i be denoted by p_i and

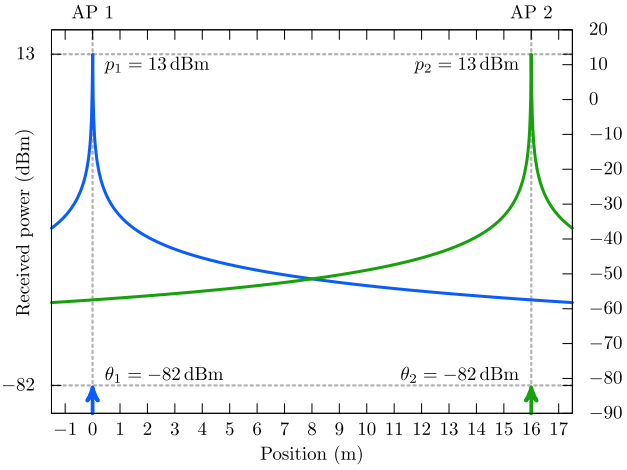

(a) Original situation, where APs 1 and 2 time-share the channel.

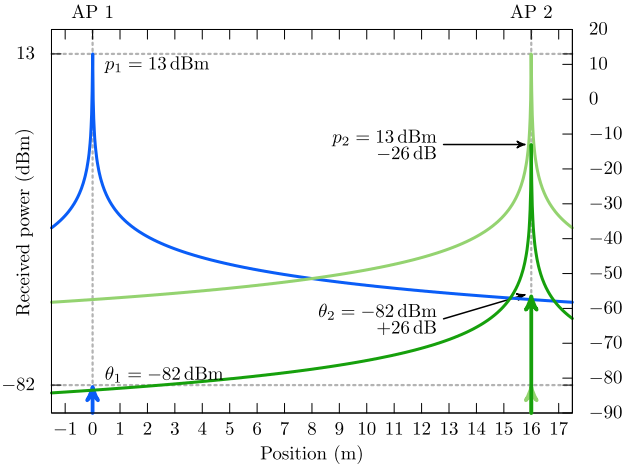

(b) AP 2 adjusts its transmission power and CST according to IPS.

Fig. 1 Carrier sensing relationship. Free space path loss is assumed.

Manuscript received September 5, 2020.
Manuscript revised January 15, 2021.
Manuscript publicized March 31, 2021.

[†]The authors are with the Graduate School of Informatics, Kyoto University, Kyoto-shi, 606-8501 Japan.
[††]The author is with the School of Engineering, Tokyo Institute of Technology, Tokyo, 158-0084 Japan.
[†††]The author is with the NTT Access Network Service Systems Laboratories, NTT Corporation, Yokosuka-shi, 239-0847 Japan.

*This paper was presented in part at IEEE CCNC 2017.

a) E-mail: kyamamot@i.kyoto-u.ac.jp

DOI: 10.1587/transcom.2020EBT0009

θ_i, respectively. As shown in Fig. 1(a), when $p_1 = 13$ dBm, the interference power at AP 2 is -58 dBm, which is greater than the CST $\theta_2 = -82$ dBm. Thus, they time-share the channel. As shown in Fig. 1(b), when AP 2 increases its CST by 26 dB to be greater than the interference power, AP 2 will transmit signals even when AP 1 transmit signals. However, AP 1 received the interference grearter than its CST θ_1, thus AP 1 should defer its transmission, i.e., APs 1 and 2 have the asymmetric carrier sensing relationship and throughput of AP 1 is starved.

To solve the problem of throughput starvation, the authors of [4], [5] proposed that each transmitter (TX) jointly tunes its CST and transmission power so that their product is equivalent to those of other TXs. This joint tuning ensures a *symmetric* carrier sensing relationship, i.e., any two TXs either detect signals from each other or they do not, and throughput starvation is thus prevented. In the example shown in Fig. 1(b), if AP 2 reduces its transmission power p_2 by 26 dB, the interference level at AP 1 is smaller than its CST θ_1, and thus, the symmetric carrier sensing relationship holds. This is called the *inversely proportional setting* (IPS) of the CST and transmission power in this paper, i.e., the transmission power is set inversely proportional to the CST. In our previous works [6], [7], we had proposed connecting attenuators between an antenna connector and an antenna for APs/STAs to achieve the IPS, and had proved the effectiveness of the IPS through experiments. The IPS is used in IEEE 802.11ax standardization [8]–[10] as well as 3GPP license assisted access (LAA) as a rule to realize fair co-existence not only among OBSSs in WLANs but also between WLANs and LAA [11].

The impact of the IPS on the system-level performance of CSMA/CA-based wireless networks should be clarified. The system-level performance of CSMA/CA networks has been analyzed based on stochastic geometry [12]–[15]. In [16]–[23], the point process of TXs at a given time was discussed mainly based on the Matérn hard-core point process (MHCPP) type II [24]. This approach enables interference modeling of CSMA/CA networks. In [20], the optimal CST was numerically provided. In [21], [23], rate adaptation was considered and a CST adaptation scheme was provided, but an explicit CST was not given. In addition, as far as the authors know, no research to date has undertaken IPS performance analysis based on stochastic geometry.

In this paper, the IPS of the CST as well as transmission power is analyzed based on stochastic geometry. Compared to previous works, the contributions are: 1) we discuss the IPS of CST and transmission power whereas previous works discussed the adjustment of CST, 2) we apply asymptotic analysis in a dense scenario to derive the optimal CST and transmission power in explicit forms, thus, we evaluate expected throughput not outage, and 3) we discuss the CST adjustment at a single TX case as well as at all TXs case. The purpose of this paper is to show the impact of IPS on throughput and optimal CST, thus, we assume the randomness is due to location of TXs and backoff time, and not to fading and maximum transmission power. We believe these simple solutions provide insight into the optimal CST according to the number of neighbors and the received signal quality, and useful for AP installations. Note that compared to our former study [25], this paper includes new Monte Carlo simulation results and revised assumptions and analytical expressions to match the simulation results. Our recent works [26], [27] analyzed the throughput based on IPS where each TX individually adjusts its CST and transmission power based on its received power by using stochastic geometry. But in these works, explicit expressions of the optimal IPS could not be derived due to fading and nearest AP association.

The rest of this paper is organized as follows. In Sect. 2, we introduce a system model and IPS. In Sect. 3, we consider adjusting a single TX. In Sect. 4, we discuss the identical adjustment at all TXs. Finally, Sect. 5 contains the conclusions of this paper.

2. System Model

2.1 Transmitters

The notation used here is shown in Table 1. We now consider a scenario where there is at most one TX-receiver (RX) pair in each basic service set (BSS) at a given time, and the set of potential TXs sharing a given channel follows a homogeneous Poisson point process (PPP) [15] Φ_p on $\mathbb{R}^2$ with density λ_p as shown as all points in Fig. 2. Note that under this assumption, all simultaneous transmissions are from OBSSs. Collisions in each BSS and multiuser transmissions are not taken into account for the sake of analysis simplic-

Table 1 Notation.

$a \coloneqq b$	a is by definition equal to b
Φ_p	PPP consisting of potential TXs with density λ_p
Φ	Point process consisting of TXs at a given time with density λ
$\Phi(S)$	Number of points of Φ inside region S
R_x	Location of RX associated with TX x
m_x	Mark, backoff time of x
$n \in \mathbb{N}$	Number of neighbors causing interference to TX x
$B \in \mathbb{R}$	Expected number of neighbors causing interference
$W(\cdot)$	Lambert W function
P	Maximum transmission power
Θ	Minimum CST
p_x, p	Transmission power of TX x
θ_x, θ	CST of TX x
a_x, a	Attenuation value of TX x
a^*	Numerically evaluated optimal a
$a^\star$	Explicit form of optimal a
α	Path loss exponent ($\alpha > 2$)
A	Constant
ρ	$\lvert S_x(a_x)\rvert/\lvert S_x(1)\rvert$
G_{xy} $(x \neq y)$	Link gain between x and y. $G_{xy} = G_{yx}$
$r(a)$	Long-term throughput per unit bandwidth of TX x
SIR_1	SIR when $a_x = 1$
$S(a)$	Contention domain of TX x depending on a
$\delta(a)$	Radius of contention domain $S(a)$
$b(x, r)$	Disk of radius r centered at x
$\#\{\cdot\}$	Number of elements of a set
$\lvert\cdot\rvert$	Area of a region
$\lVert\cdot\rVert$	Euclidean distance

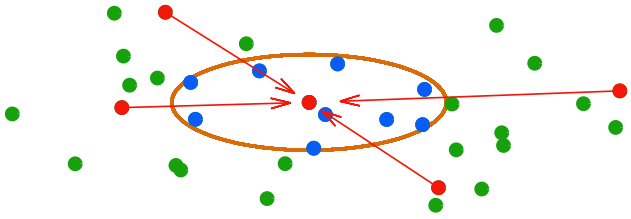

(a) Before applying IPS ($a = 1$). The red point in the center time-shares the channel with blue points.

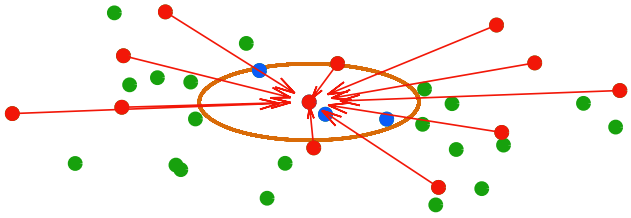

(b) After applying IPS ($a > 1$). The number of blue points are reduced, thus, the medium access probability is increased. In contrast, the number of interference sources increases.

Fig. 2 Impact of IPS. Orange circle: contention domain $S(a)$, all points: potential TXs Φ_p, blue points: $\Phi_\mathrm{p} \cap S(a)$, red points: TXs at a given time Φ and receives interference from other red points.

ity. Let the transmission power and CST of TX $x \in \Phi_\mathrm{p}$ be denoted by p_x and θ_x, respectively. As in [19], to clarify the relationship among the CST, throughput, and density, we assume that the sources of randomness are the location of the TXs and backoff time.

TX x defers its transmission if backoff time of TX $z \in \Phi_\mathrm{p} \setminus \{x\}$ is smaller than that of x and received interference power is greater than the CST, i.e.,

$$G_{xz} p_z > \theta_x, \tag{1}$$

where G_{xz} represents the link gain between TXs x and z; it is assumed to be given by

$$G_{xz} = A\|x - z\|^{-\alpha}, \tag{2}$$

where $\|\cdot\|$ represents Euclidean distance, α represents the path loss exponent ($\alpha > 2$), and A is a constant. Note that (2) implies that the link gain is symmetric, i.e., $G_{xz} = G_{zx}$.

2.2 Inversely Proportional Setting of CST and Transmission Power

To avoid throughput starvation due to the asymmetric carrier sensing relationship, Mhatre et al. [4] proposed that each TX jointly adjusts its CST and transmission power in order for their product to be equal to those of others. Here, in order to take into account legacy devices that do not have functionality of CST and transmission power adjustment, we consider an IPS such that

$$p_x \theta_x = P\Theta, \ \forall x \in \Phi_\mathrm{p}, \tag{3}$$

where Θ and P represent the CST and transmission power of legacy devices. For ease of expression, we introduce an auxiliary variable a_x satisfying (3) as

$$\theta_x = \Theta a_x, \ p_x = P/a_x, \tag{4}$$

where a_x (≥ 1) represents ratios θ_x/Θ and P/p_x.

3. Adjustment at a Single Transmitter

3.1 Medium Access Probability

We first discuss a simple scenario where only one TX $x \in \Phi_\mathrm{p}$ adjusts its CSTθ_x, transmission power p_x, and a_x, whereas other TXs utilize the minimum CST and maximum transmission power, i.e., $\theta_z = \Theta$, $p_z = P$, and $a_z = 1$ for all $z \in \Phi_\mathrm{p} \setminus \{x\}$. For notational convenience, hereinafter we simply use p, θ, and a for p_x, θ_x, and a_x, respectively. Here, we introduce the contention domain of TX x as

$$S(a) \coloneqq \{ z \in \mathbb{R}^2 \setminus \{x\} \mid G_{xz} P > \theta \}. \tag{5}$$

Note that $S(1)$ represents the contention domain when $a = 1$, i.e., $\theta = \Theta$ and $p = P$. Figure 2 shows an impact of IPS by adjusting a, i.e., the size of contention domain $S(a)$. Let $\Phi_\mathrm{p}(S)$ represent the number of points of Φ_p in region S.

We consider the setting of a based only on the number of neighboring potential TXs when $a = 1$, $n = \Phi_\mathrm{p}(S(1))$. Note that n is a natural number. We also assume that n TXs are uniformly and independently distributed in $S(1)$, i.e., the set of potential TXs follows a binomial point process (BPP) [12].

Lemma 1: The distribution of the number of neighboring potential TXs when applying IPS, $\Phi_\mathrm{p}(S(a))$ for $a \geq 1$, is given by

$$\begin{aligned}&\mathbb{P}(\Phi_\mathrm{p}(S(a)) = k \mid \Phi_\mathrm{p}(S(1)) = n) \\ &\quad = \binom{n}{k} (a^{-2/\alpha})^k (1 - a^{-2/\alpha})^{n-k},\end{aligned} \tag{6}$$

for $k = 0, 1, \ldots, n$.

Proof 1: Since we assume that the set of potential TXs follows a BPP, the distribution is given by

$$\mathbb{P}(\Phi_\mathrm{p}(S(a)) = k \mid \Phi_\mathrm{p}(S(1)) = n) = \binom{n}{k} \rho^k (1 - \rho)^{n-k}, \tag{7}$$

where

$$\rho \coloneqq \frac{|S(a)|}{|S(1)|} \tag{8}$$

and $|\cdot|$ represents the area of the region [15, Theorem 2.9]. To evaluate (7), we need to discuss ρ. Substituting (2) and (4) into (5), we get

$$S(a) = \{ z \in \mathbb{R}^2 \setminus \{x\} \mid \|z - x\| < (AP/\Theta a)^{1/\alpha} \}. \tag{9}$$

Thus, the radius of $S(a)$ is $\delta(a) = (AP/\Theta a)^{1/\alpha}$, and

$$\rho = \frac{|S(a)|}{|S(1)|} = \frac{\pi\delta(a)^2}{\pi\delta(1)^2} = a^{-2/\alpha}. \tag{10}$$

Substituting (10) into (7), we get (6). □

Let backoff time of each potential TX $x \in \Phi_\mathrm{p}$ be denoted by m_x and it is assumed that m_x is an independent random variable uniformly distributed on $[0, 1]$ as in [14, Sect. 18]. TX x would transmit if $m_x < m_z$ for all $z \in \Phi_\mathrm{p} \cap S(a)$.

Lemma 2: When $\Phi_\mathrm{p}(S(1)) = n$, the medium access probability for $a \geq 1$ is given by

$$MAP(a, n) = \frac{1 - (1 - a^{-2/\alpha})^{n+1}}{(n+1)a^{-2/\alpha}}, \tag{11}$$

where ρ is defined in Lemma 1.

Proof 2: Since in contention domain $S(a)$, the probability that backoff time is less than t is given by $ta^{-2/\alpha}$, substituting $\rho = ta^{-2/\alpha}$ into (7), and evaluate the probability that there are no points in $S(a)$, we get

$$\begin{aligned} MAP(a, n) &= \int_0^1 \mathbb{P}(\Phi_\mathrm{p}(S(a)) = 0 \mid \Phi_\mathrm{p}(S(1)) = n)\,\mathrm{d}t \\ &= \int_0^1 (1 - ta^{-2/\alpha})^n\,\mathrm{d}t \\ &= \frac{1 - (1 - a^{-2/\alpha})^{n+1}}{(n+1)a^{-2/\alpha}}. \end{aligned}$$ □

We then discuss an asymptotic expression in a dense scenario.

Proposition 1: As $\lambda_\mathrm{p} \to \infty$,

$$MAP(a, n) \simeq \frac{1}{1 + na^{-2/\alpha}} =: MAP'(a, n) \tag{12}$$

Proof 3: As $\lambda_\mathrm{p} \to \infty$, $n \to \infty$,

$$\lim_{n\to\infty}\left[\frac{1 - (1 - a^{-2/\alpha})^{n+1}}{(n+1)a^{-2/\alpha}} - \frac{1}{1 + na^{-2/\alpha}}\right] = 0.$$ □

3.2 Interference and SIR

Let the location of RX associated with TX $x \in \Phi_\mathrm{p}$ be denoted by $R_x \in \mathbb{R}^2$. The interference-plus-noise power level at R_x is assumed to be approximate to that at TX x, and it is also assumed to be approximate to the CST θ as in [4] (hereinafter referred to as the "SIR approximation"). This assumption is reasonable because the interference level is guaranteed to be less than the CST due to the carrier sense mechanism. In this case, the signal-to-interference power ratio (SIR) is given by

$$SIR(a) \coloneqq \frac{G_{R_x x} p}{\theta} = \frac{G_{R_x x} P}{\Theta a^2} = \frac{SIR_1}{a^2}, \tag{13}$$

where $SIR_1 \coloneqq G_{R_x x} P/\Theta$ represents SIR when $a = 1$.

The SIR approximation is equivalent to the approximation that the nearest TX is on the border of $S(a)$, thus, it underestimates the distance and results in underestimation of the SIR (13). To compensate them, we discuss the nearest neighbor distance after applying IPS. In Sect. 3.1, we consider the situation where n TXs are in $S(1)$ before applying IPS. For the ease of evaluation, we assume a PPP Φ' with the same density,

$$\lambda' \coloneqq \frac{n}{|S(1)|} \tag{14}$$

outside the contention domain $S(a)$. According to [15, 2.9.1], the distribution of the distance to the nearest TX in $\Phi' \setminus S(a)$ is given by

$$\begin{aligned} G(r) &= 1 - \mathbb{P}(\Phi'(b(x, r) \setminus S(a)) = 0) \\ &= 1 - \exp(-\lambda'\pi(r^2 - \delta(a)^2)),\ r > \delta(a) \end{aligned} \tag{15}$$

$$g(r) \coloneqq \frac{\mathrm{d}}{\mathrm{d}r}G(r) = 2\lambda'\pi r \exp(-\lambda'\pi(r^2 - \delta(a)^2)), \tag{16}$$

where $b(x, r)$ represents a disk of radius r centered at x. Thus, the expected distance is given by

$$\begin{aligned} \mathbb{E}[r] &= \int_{\delta(a)}^{\infty} r\, g(r)\,\mathrm{d}r \\ &= \delta(a) + \frac{\sqrt{\pi}\delta(1)}{2\sqrt{n}} \exp(na^{-2/\alpha})\,\mathrm{erfc}\sqrt{na^{-2/\alpha}}. \end{aligned} \tag{17}$$

Finally, to compensate the underestimation, the nearest neighbor distance should be reduced from $\delta(a)$ to $\mathbb{E}[r]$. In this case, the SIR is estimated by

$$\begin{aligned} SIR'(a) &\coloneqq SIR(a)\,\frac{A\delta(a)^{-\alpha}}{A(\mathbb{E}[r])^{-\alpha}} \\ &= \frac{SIR_1}{a^2}\left[1 + \frac{\sqrt{\pi}a^{1/\alpha}}{2\sqrt{n}} \exp(na^{-2/\alpha})\,\mathrm{erfc}\sqrt{na^{-2/\alpha}}\right]^{\alpha}. \end{aligned} \tag{18}$$

3.3 Throughput Modeling

We evaluate the long-term throughput of WLANs under saturated traffic conditions and interference-limited situations by the product of the medium access probability (11) and Shannon capacity with SIR (18) assuming that interference is equivalent to Gaussian noise,

$$r(a) \coloneqq MAP(a, n) \cdot \log_2(1 + SIR'(a)). \tag{19}$$

The IPS reduces the number of neighboring potential TXs while also reducing SIR. That is, there is a trade-off between the number of neighboring potential TXs and SIR, and the careful adjustment of parameter a is required to achieve high throughput.

If we set the value of parameters α, n, and SIR_1, we can numerically find the optimal value $a^* \coloneqq \arg\max_a r(a)$, i.e., the optimal CST Θa^* and transmission power P/a^*, but an explicit expression for a^* cannot be derived.

3.4 Explicit Expression of Optimal CST and Transmission Power

To achieve an explicit solution, we first use the SIR approximation, i.e.,

$$r(a) \approx MAP(a,n) \cdot \log_2(1 + SIR(a)), \tag{20}$$

and then discuss the asymptotic expression in a dense scenario. As $\lambda_p \to \infty$,

$$(20) \simeq MAP'(a,n) \cdot \log_2(1 + SIR(a)). \tag{21}$$

In addition, assuming a high SIR regime, we can ignore the fixed value, 1, inside the logarithm in (21) and get

$$\begin{aligned}(21) &\approx MAP'(a,n) \cdot \log_2(SIR(a)) \\ &= \frac{\log_2(SIR_1/a^2)}{1 + na^{-2/\alpha}}.\end{aligned} \tag{22}$$

(22) is useful for attaining the optimal solution, as shown in Proposition 2.

Proposition 2: The unique maximum of (22) is attained at

$$\begin{aligned}a^\star &:= \arg\max_a \frac{\log_2(SIR_1/a^2)}{1 + na^{-2/\alpha}} \\ &= \max\{[nW({SIR_1}^{1/\alpha}/en)]^{\alpha/2}, 1\},\end{aligned} \tag{23}$$

i.e., at CST $\Theta a^\star$ and transmission power $P/a^\star$, where $W(\cdot)$ represents the principal branch of the Lambert W function [28].

Proof 4: The result follows from (22) by differentiation with respect to a. Following a few manipulations, we get

$$(a^{\star 2/\alpha}/n)\exp(a^{\star 2/\alpha}/n) = {SIR_1}^{1/\alpha}/en.$$

Using the Lambert W function, defined as the inverse of function $w \mapsto w\exp(w)$ [28], we get

$$a^{\star 2/\alpha}/n = W({SIR_1}^{1/\alpha}/en).$$

Since $a \geq 1$, we get (23). □

3.5 Numerical Evaluation

Figure 3 shows numerical examples of throughput (19). It also presents results of Monte Carlo simulations with 10,000 trials, where we determine the location of RX associated with x so that the SIR is equal to SIR_1. Although there is a gap between the numerical results (19) and simulation results, we can confirm a similar trend and there is a unique optimal value in terms of throughput. The gap is due to the SIR approximation and some of the assumptions used to derive $SIR'(a)$ in (18).

Figure 3 also shows the approximated throughput (20)–(22). As has been discussed, the approximation is valid for high SIR regions, i.e., when a is sufficiently low to maintain

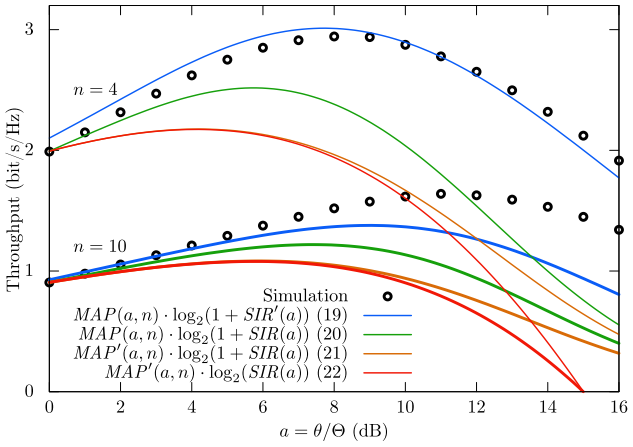

Fig. 3 Throughput (19)–(22). $SIR_1 = 30$ dB, $\alpha = 3.5$.

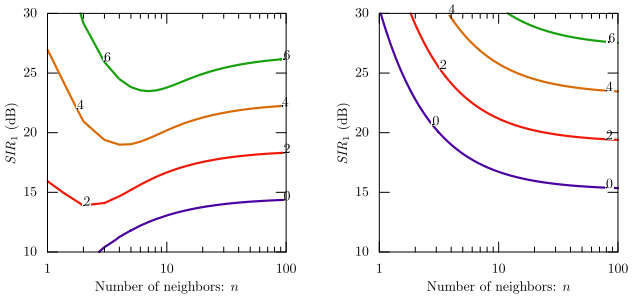

(a) Numerically achieved optimal value a^*.

(b) Explicit solution of approximated throughput $a^\star$.

Fig. 4 Contour plot of optimal value in dB in terms of throughput. $\alpha = 3.5$.

$SIR_1/a^2 \gg 1$.

Figure 4(a) shows the contour plot of the numerically calculated optimal value a^* in terms of throughput (19). We can see that a^* depends both on the number of neighbors n and SIR_1, i.e., SIR at $a = 0$ dB. Figure 4(b) shows the explicit expression $a^\star$ (23).

To confirm the effectiveness of (23) in terms of throughput estimation, Fig. 5 shows the contour plot of the following normalized loss due to approximation:

$$\frac{r(a^*) - r(a^\star)}{r(a^*)}. \tag{24}$$

The maximum loss is 15% for $10 \leq n \leq 100$ and $10\,\text{dB} \leq SIR_1 \leq 30\,\text{dB}$. Thus, we can conclude that the explicit expression (23) is useful for the IPS of the CST and transmission power for these situations.

4. Adjustment at All Transmitters

4.1 Medium Access Probability

We now consider a scenario where all TXs are assumed to set the identical CST and transmission power according to IPS, i.e., $p_x = p$, $\theta_x = \theta$, and $a_x = a$ for every $x \in \Phi_p$. In addition, we assume a Poisson bipolar model as in [19], [20],

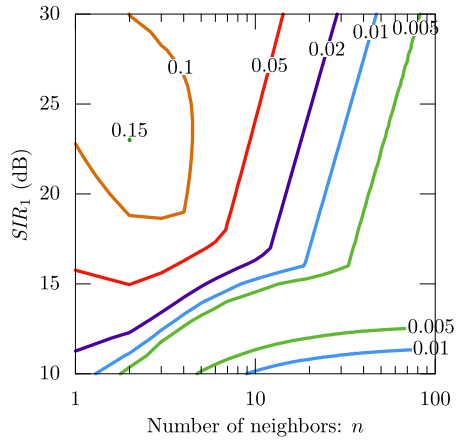

Fig. 5 Contour plot of loss due to approximation (24). The maximum loss is 0.15 for this region.

where $G_{R_x x} = G_{R_y y}$ for all x and y in Φ_p. Note that these simplified assumptions are intended to achieve simple but insightful expressions for the throughput and the optimal value of the CST.

At a given time, it is assumed that the set of simultaneously transmitting APs is modeled as an MHCPP Φ [24] as in [16], [29], which is generated by dependent thinning of Φ_p as follows. The potential TX $x \in \Phi_\mathrm{p}$ is retained if $m_x < m_z$ for all $z \in \Phi_\mathrm{p} \cap S(a)$, where $S(a)$ represents the contention domain of TX x:

$$\begin{aligned} S(a) &:= \{\, z \in \mathbb{R}^2 \setminus \{x\} \mid G_{xz} p > \theta \,\} \\ &= \{\, z \in \mathbb{R}^2 \setminus \{x\} \mid G_{xz} P > \Theta a^2 \,\}. \end{aligned} \tag{25}$$

The radius of $S(a)$ is $\delta(a) := (AP/\Theta a^2)^{1/\alpha} = \delta(1)\, a^{-2/\alpha}$. Note that $\delta(a)$ is different from that in Sect. 3.

Let the density of Φ be denoted by λ. The retaining probability of point $x \in \Phi_\mathrm{p}$, i.e., the medium access probability, is given by [24], [14, (18.5)], [30]

$$MAP(a) := \frac{\lambda}{\lambda_\mathrm{p}} = \frac{1 - \exp(-\lambda_\mathrm{p} |S(a)|)}{\lambda_\mathrm{p} |S(a)|}, \tag{26}$$

where

$$\begin{aligned} \lambda_\mathrm{p} |S(a)| &= \lambda_\mathrm{p} |\{\, z \in \mathbb{R}^2 \setminus \{x\} \mid G_{zx} P > \Theta a^2 \,\}| \\ &= \lambda_\mathrm{p} |\{\, z \in \mathbb{R}^2 \setminus \{x\} \mid A \|z - x\|^{-\alpha} P > \Theta a^2 \,\}| \\ &= \lambda_\mathrm{p} \pi (AP/\Theta a^2)^{2/\alpha} = B a^{-4/\alpha}, \end{aligned} \tag{27}$$

where $B := \lambda_\mathrm{p} \pi (AP/\Theta)^{2/\alpha} = \mathbb{E}[\Phi_\mathrm{p}(S(1))]$ represents the expected number of neighbors. Note that B is a positive real value, whereas n defined in Sect. 3 is a natural number.

As in Sect. 3, we consider a dense scenario.

Proposition 3: As $\lambda_\mathrm{p} \to \infty$,

$$MAP(a) \simeq \frac{1}{1 + B a^{-4/\alpha}} =: MAP'(a). \tag{28}$$

Proof 5: Similar to that of Proposition 1. □

4.2 Interference and SIR

The average interference at RX R_x is approximated by the average interference at TX x, and we assume x is at the origin o without loss of generality:

$$\begin{aligned} I(a) &:= \mathbb{E}\left[\sum_{z \in \Phi_\mathrm{p} \setminus S(a)} G_{R_x z} p \right] \approx \mathbb{E}\left[\sum_{z \in \Phi_\mathrm{p} \setminus S(a)} G_{oz} p \right] \\ &= \frac{AP}{a} \mathbb{E}\left[\sum_{z \in \Phi_\mathrm{p} \setminus S(a)} \|z\|^{-\alpha} \right] \\ &\overset{\text{(a)}}{=} \frac{AP\lambda_\mathrm{p}}{a} \int_{\mathbb{R}^2 \cap (\|z\| \geq \delta(a))} \|z\|^{-\alpha} \, \mathrm{d}z \\ &= \frac{AP 2\pi\lambda_\mathrm{p}}{a} \int_{\delta(a)}^{\infty} r^{1-\alpha} \, \mathrm{d}r = \frac{AP 2\pi\lambda_\mathrm{p}}{a(\alpha - 2)} \delta(a)^{2-\alpha}, \end{aligned} \tag{29}$$

where transformation (a) follows the Campbell's theorem [15]. Therefore, the average interference is reduced by the following factor

$$\frac{I(a)}{I(1)} = \frac{1}{a} \left(\frac{\delta(a)}{\delta(1)} \right)^{2-\alpha} = a^{-1} (a^{-2/\alpha})^{2-\alpha} = a^{1-4/\alpha}. \tag{30}$$

Also, desired signal level is reduced by factor $1/a$ due to IPS. Therefore, the SIR after IPS is given by

$$SIR(a) := SIR_1 \frac{1/a}{a^{1-4/\alpha}} = SIR_1\, a^{4/\alpha - 2}, \tag{31}$$

where SIR_1 represents the SIR when $a = 1$ as has been defined in Sect. 3.

4.3 Throughput Modeling

As with (19) in the single TX adjustment scenario, individual throughput is given by

$$\begin{aligned} r(a) &:= MAP(a) \log_2(1 + SIR(a)) \\ &= \frac{1 - \exp(-B a^{-4/\alpha})}{B a^{-4/\alpha}} \log_2(1 + SIR_1 a^{4/\alpha - 2}). \end{aligned} \tag{32}$$

Note that the differences between the adjustment at a single TX discussed in Sect. 3 and that of all TXs are: 1) BPP is used in Sect. 3, whereas PPP is used in Sect. 4, and 2) the contention domain is reduced by a factor of $a_x{}^{-2/\alpha}$ in Sect. 3, but by a factor of $a^{-4/\alpha}$ in Sect. 4 because the surrounding TXs also reduce their transmission power.

4.4 Optimal CST and Transmission Power

We would like to find the optimal value of a that maximizes expected throughput, i.e., $a^* = \arg\max_a r(a)$. We thus consider the approximated throughput of (32) assuming a high SIR and dense regime

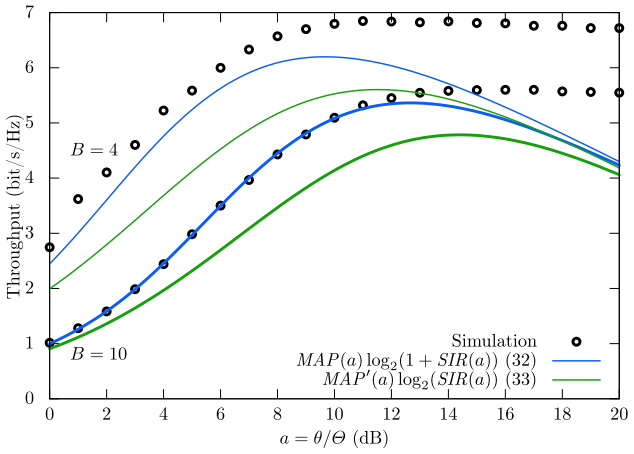

Fig. 6 Throughput: (32) and its approximation: (33). $SIR_1 = 30$ dB, $\alpha = 3.5$.

$$r(a) \approx MAP'(a)\log_2(SIR(a)) = \frac{\log_2(SIR_1 a^{4/\alpha-2})}{1 + Ba^{-4/\alpha}}. \quad (33)$$

Proposition 4: The unique maximum of (33) is attained at

$$a^\star = \max\left\{\left[B\,W\left(\frac{{SIR_1}^{2/(\alpha-2)}}{eB}\right)\right]^{\alpha/4}, 1\right\}. \quad (34)$$

This condition is equivalent to $p^\star = P/a^\star$ and $\theta^\star = \Theta a^\star$.

Proof 6: The approach is the same as the one adopted in the proof of Proposition 2. Differentiating (33) with respect to a and following some manipulations, we get

$$\frac{a^{\star 4/\alpha}}{B}\exp\left(\frac{a^{\star 4/\alpha}}{B}\right) = \frac{{SIR_1}^{2/(\alpha-2)}}{eB}.$$

Using the Lambert W function,

$$\frac{a^{\star 4/\alpha}}{B} = W\left(\frac{{SIR_1}^{2/(\alpha-2)}}{eB}\right).$$

Taking $a \geq 1$ into account, we get (34). □

4.5 Numerical Evaluation

Figure 6 shows the throughput (32) and its approximation (33) for deriving the optimal setting as shown in Proposition 4. It also presents Monte Carlo simulation results with 1,000 trials. We can see that all of these have a unique maximum. Although the difference between the throughput and its asymptotic throughput is not small, they have maximum values around $a^\star$ given by (34). Thus, we can conclude that despite approximations, (34) can be used for the CST and transmission power setting to achieve high throughput.

Figure 7 shows a^* and $a^\star$, and we can see the similarity in trends. Similarly to (24), we calculated the normalized loss $[r(a^*) - r(a^\star)]/r(a^*)$ as shown in Fig. 8. We confirmed that the loss was less than 10% for high SIR condition

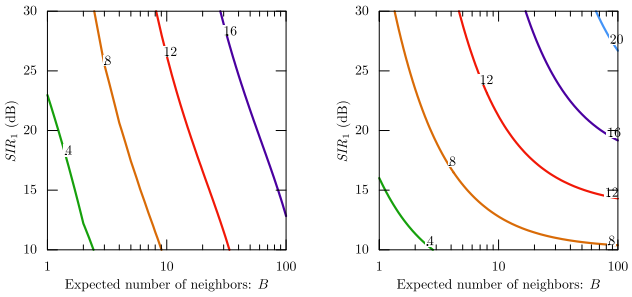

(a) Numerically optimized value a^*. (b) Explicit solution $a^\star$ (34).

Fig. 7 Optimal attenuation value in dB in terms of throughput. $\alpha = 3.5$.

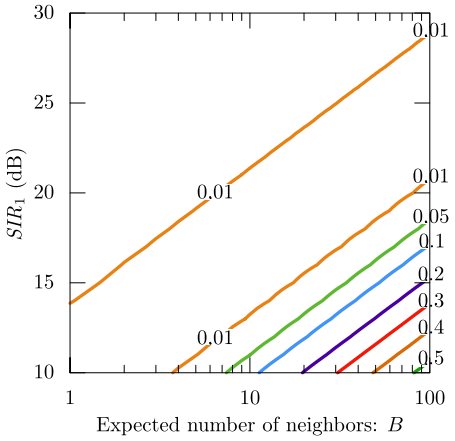

Fig. 8 Contour plot of loss due to approximation, $[r(a^*)-r(a^\star)]/r(a^*)$. $\alpha = 3.5$.

($SIR_1 > 21$ dB). Thus, the explicit solution $a^\star$ provides a satisfactory guideline for designing the IPS.

5. Conclusion

In this paper, we discussed the joint adjustment of CST and transmission power. Throughput was formulated by assuming that the set of potential TXs forms a PPP. The explicit expressions of the optimal IPS of the CST and transmission power in term of throughput were obtained as a function of SIR and the number of neighbors. Numerical results confirmed that the explicit solutions are applicable to the inversely proportional setting despite approximations.

References

[1] IEEE Std 802.11-2016, "Part 11: Wireless LAN medium access control (MAC) and physical layer (PHY) specifications," Dec. 2016.
[2] J. Zhu, X. Guo, L.L. Yang, W.S. Conner, S. Roy, and M.M. Hazra, "Adapting physical carrier sensing to maximize spatial reuse in 802.11 mesh networks," Wirel. Commun. Mob. Comput., vol.4, no.8, pp.933–946, Dec. 2004.
[3] M.S. Afaqui, E. Garcia-Villegas, E. Lopez-Aguilera, G. Smith, and D. Camps, "Evaluation of dynamic sensitivity control algorithm for IEEE 802.11ax," Proc. IEEE Wireless Commun. Netw. Conf. (WCNC), New Orleans, LA, pp.1060–1065, March 2015.
[4] V.P. Mhatre, K. Papagiannaki, and F. Baccelli, "Interference mitigation through power control in high density 802.11 WLANs," Proc.

IEEE Int. Conf. Comput. Commun. (INFOCOM), Anchorage, AK, pp.535–543, May 2007.
[5] J.A. Fuemmeler, N.H. Vaidya, and V.V. Veeravalli, "Selecting transmit powers and carrier sense thresholds in CSMA protocols for wireless ad hoc networks," Proc. Int. Wireless Internet Conf. (WICON), New York, NY, USA, Aug. 2006.
[6] D. Okuhara, F. Shiotani, K. Yamamoto, T. Nishio, M. Morikura, R. Kudo, and K. Ishihara, "Attenuators enable inversely proportional transmission power and carrier sense threshold setting in WLANs," Proc. 25th IEEE Int. Symp. Personal, Indoor and Mobile Radio Commun. (PIMRC), Washington, DC, USA, pp.986–990, Sept. 2014.
[7] D. Okuhara, K. Yamamoto, T. Nishio, M. Morikura, and H. Abeysekera, "Inversely proportional transmission power and carrier sense threshold setting for WLANs: Experimental evaluation of partial settings," Proc. IEEE Veh. Tech. Conf. (VTC2016-Fall), Montreal, Canada, pp.1–5, Sept. 2016.
[8] IEEE P802.11ax/D7.0, "Wireless LAN medium access control (MAC) and physical layer (PHY) specifications amendment enhancements for high efficiency WLAN," Sept. 2020.
[9] Y. Asai, "Advanced progress in IEEE 802.11 WLAN standardization," Proc. Asia-Pacific Microwave Conf. (APMC), Sendai, Japan, pp.911–913, Nov. 2014.
[10] F. Wilhelmi, S.B. Muñoz, C. Cano, I. Selinis, and B. Bellalta, "Spatial reuse in IEEE 802.11ax WLANs," arXiv: 1907.04141, Nov. 2019.
[11] J. Wang et al., "Adjustment rules for adaptive CCA and TPC," IEEE 802.11-16/0414r1, March 2016.
[12] S.N. Chiu, D. Stoyan, W. Kendall, and J. Mecke, Stochastic Geometry and Its Applications, 3rd ed., John Wiley & Sons, 2013.
[13] F. Baccelli and B. Blaszczyszyn, "Stochastic geometry and wireless networks: Volume I theory," Found. Trends Netw., vol.3, no.3-4, pp.249–449, 2009.
[14] F. Baccelli and B. Blaszczyszyn, "Stochastic geometry and wireless networks: Volume II applications," Found. Trends Netw., vol.4, no.1-2, pp.1–312, 2009.
[15] M. Haenggi, Stochastic Geometry for Wireless Networks, Cambridge Univ. Press, Cambridge, U.K., 2012.
[16] H.Q. Nguyen, F. Baccelli, and D. Kofman, "A stochastic geometry analysis of dense IEEE 802.11 networks," Proc. IEEE Int. Conf. Comput. Commun. (INFOCOM), Anchorage, AK, pp.1199–1207, May 2007.
[17] A. Busson and G. Chelius, "Point processes for interference modeling in CSMA/CA ad-hoc networks," Proc. the 6th ACM Symp. Perform. Eval. Wireless Ad Hoc, Sensor, Ubiquitous Netw. (PE-WASUN), Canary Islands, Spain, p.33, Oct. 2009.
[18] G. Alfano, M. Garetto, and E. Leonardi, "New insights into the stochastic geometry analysis of dense CSMA networks," Proc. IEEE Int. Conf. Comput. Commun. (INFOCOM), Shanghai, China, pp.2642–2650, April 2011.
[19] M. Kaynia, N. Jindal, and G.E. Oien, "Improving the performance of wireless ad hoc networks through MAC layer design," IEEE Trans. Wireless Commun., vol.10, no.1, pp.240–252, Jan. 2011.
[20] H. ElSawy and E. Hossain, "A modified hard core point process for analysis of random CSMA wireless networks in general fading environments," IEEE Trans. Commun., vol.61, no.4, pp.1520–1534, April 2013.
[21] D.M. Kim and S.L. Kim, "An iterative algorithm for optimal carrier sensing threshold in random CSMA/CA wireless networks," IEEE Commun. Lett., vol.17, no.11, pp.2076–2079, Nov. 2013.
[22] G. Alfano, M. Garetto, and E. Leonardi, "New directions into the stochastic geometry analysis of dense CSMA networks," IEEE Trans. Mobile Comput., vol.13, no.2, pp.324–336, Feb. 2014.
[23] Z. Zhang, Y. Li, K. Huang, and C. Liang, "On stochastic geometry modeling of WLAN capacity with dynamic sensitive control," Proc. Int. Symp. Model. Optim. Mobile Ad Hoc Wireless Netw. (WiOpt), Mumbai, India, pp.78–83, May 2015.
[24] B. Matérn, Spatial Variation, 2nd ed., Springer-Verlag, 1986.
[25] K. Yamamoto, X. Yang, T. Nishio, M. Morikura, and H. Abeysekera, "Analysis of inversely proportional carrier sense threshold and transmission power setting," Proc. IEEE Consum. Commun. Netw. Conf. (CCNC), Las Vegas, NV, USA, Jan. 2017.
[26] M. Iwata, K. Yamamoto, B. Yin, T. Nishio, M. Morikura, and H. Abeysekera, "Analysis of inversely proportional carrier sense threshold and transmission power setting based on received power for IEEE 802.11ax," Proc. IEEE Consum. Commun. Netw. Conf. (CCNC), Las Vegas, NV, USA, pp.1–6, Jan. 2019.
[27] M. Iwata, K. Yamamoto, B. Yin, T. Nishio, M. Morikura, and H. Abeysekera, "Stochastic geometry analysis of individual carrier sense threshold adaptation in IEEE 802.11ax WLANs," IEEE Access, vol.7, pp.161916–161927, Nov. 2019.
[28] R.M. Corless, G.H. Gonnet, D.E.G. Hare, D.J. Jeffrey, and D.E. Knuth, "On the Lambert w function," Adv. Comput. Math., vol.5, no.1, pp.329–359, Dec. 1996.
[29] H. ElSawy, E. Hossain, and S. Camorlinga, "Characterizing random CSMA wireless networks: A stochastic geometry approach," Proc. IEEE Int. Conf. Commun. (ICC), Ottawa, ON, pp.5000–5004, June 2012.
[30] M. Haenggi, "Mean interference in hard-core wireless networks," IEEE Commun. Lett., vol.15, no.8, pp.792–794, Aug. 2011.

Koji Yamamoto received the B.E. degree in electrical and electronic engineering from Kyoto University in 2002, and the master and Ph.D. degrees in Informatics from Kyoto University in 2004 and 2005, respectively. From 2004 to 2005, he was a research fellow of the Japan Society for the Promotion of Science (JSPS). Since 2005, he has been with the Graduate School of Informatics, Kyoto University, where he is currently an associate professor. From 2008 to 2009, he was a visiting researcher at Wireless@KTH, Royal Institute of Technology (KTH) in Sweden. He serves as an editor of IEEE Open Journal of Vehicular Technology, IEEE Wireless Communications Letters, and Journal of Communications and Information Networks, a track co-chair of APCC 2017, CCNC 2018, APCC 2018, and CCNC 2019, and a vice co-chair of IEEE ComSoc APB CCC. He was a tutorial lecturer in IEEE ICC 2019. His research interests include radio resource management, game theory, and machine learning. He received the PIMRC 2004 Best Student Paper Award in 2004, the Ericsson Young Scientist Award in 2006. He also received the Young Researcher's Award, the Paper Award, SUEMATSU-Yasuharu Award, Educational Service Award from the IEICE of Japan in 2008, 2011, 2016, and 2020, respectively, and IEEE Kansai Section GOLD Award in 2012. He is a senior member of the IEEE and a member of the Operations Research Society of Japan.

Takayuki Nishio is an associate professor at the School of Engineering, Tokyo Institute of Technology, Japan. He received the B.E. degree in electrical and electronic engineering and the master's and Ph.D. degrees in informatics from Kyoto University in 2010, 2012, and 2013, respectively. He was an assistant professor in communications and computer engineering with the Graduate School of Informatics, Kyoto University from 2013 to 2020. From 2016 to 2017, he was a visiting researcher in Wireless Information Network Laboratory (WINLAB), Rutgers University, United States. His current research interests include machine learning-based network control, machine learning in wireless networks, vision-aided wireless communications, and heterogeneous resource management.

Masahiro Morikura received B.E., M.E. and Ph.D. degree in electronic engineering from Kyoto University, Kyoto, Japan in 1979, 1981 and 1991, respectively. He joined NTT in 1981, where he was engaged in the research and development of TDMA equipment for satellite communications. From 1988 to 1989, he was with the communications Research Centre, Canada as a guest scientist. From 1997 to 2002, he was active in standardization of the IEEE802.11a based wireless LAN. He received Paper Award, Achievement Award and Distinguished Achievement and Contributions Award from the IEICE in 2000, 2006 and 2019, respectively. He also received Education, Culture, Sports, Science and Technology Minister Award in 2007 and Maejima Award from the Teishin association in 2008 and the Medal of Honor with Purple Ribbon from Japan's Cabinet Office in 2015. Dr. Morikura is now a professor of the Graduate School of Informatics, Kyoto University. He is a Fellow of the IEICE and a member of IEEE.

Hirantha Abeysekera received the B.Eng., M.Eng., and Ph.D. degrees in communications engineering from Osaka University, Japan, in 2005, 2007, and 2010, respectively. In 2010, he joined NTT Network Innovation Laboratories, Yokosuka, Japan. He has been engaged in the research and development of next-generation wireless LAN systems. He received the IEEE VTS Japan Student Paper award in 2009. He is a member of the IEEE.